Harmful Algae
November 2021, Volume 109 Pages 102107 (13p.)
https://doi.org/10.1016/j.hal.2021.102107
https://archimer.ifremer.fr/doc/00725/83681/

A new potentially toxic dinoflagellate *Fukuyoa koreansis* sp. nov. (Gonyaulacales, Dinophyceae) from Korean coastal waters: Morphology, phylogeny, and effects of temperature and salinity on growth

Li Zhun [1], Park Joon Sang [2], Kang Nam Seon [3], Chomérat Nicolas [4], Mertens Kenneth [4], Gu Haifeng [5], Lee Kyun-Woo [6], Kim Ki Hyun [1], Baek Seung Ho [7], Shin Kyoungsoon [8], Han Kyong Ha [2], Son Moon Ho [9], Shin Hyeon Ho [2, *]

[1] Biological Resource Center/Korean Collection for Type Cultures (KCTC), Korea Research Institute of Bioscience and Biotechnology, Jeongeup 56212, Republic of Korea
[2] Library of Marine Samples, Korea Institute of Ocean Science & Technology, Geoje 53201, Republic of Korea
[3] Marine Biodiversity Institute of Korea, Seocheon 33662, Republic of Korea
[4] Ifremer, LITTORAL, F-29900 Concarneau, France
[5] Third Institute of Oceanography, Ministry of Natural Resources, Xiamen 361005, China
[6] Marine Ecosystem and Biological Research Center, Korea Institute of Ocean Science & Technology, Republic of Korea
[7] Risk Assessment Research Center, Korea Institute of Ocean Science & Technology, Geoje 53201, Republic of Korea
[8] Ballast Water Research Center, Korea Institute of Ocean Science & Technology, Geoje 53201, Republic of Korea
[9] National Institute of Fisheries Science, Busan, 619-705, Republic of Korea

* Corresponding author : Hyeon Ho Shin, email address : shh961121@kiost.ac.kr

Abstract :

To clarify an unspecified toxic Gambierdiscus-like species isolated from seawaters off Jeju Island, Korea, its morphology and molecular phylogeny based on the small subunit (SSU) and partial large subunit (LSU) rRNA gene sequences were examined. Cells were narrow in ventral view and broad in lateral view with a smooth surface. The round thecal pores were evenly distributed, with an average diameter of 0.41 µm. Cell depth, width and height were 51.7 ± 4.5 µm, 43.0 ± 4.2 µm and 55.0 ± 4.7 µm, respectively, and depth-to-width (D/W) and height-to-width (H/W) ratios were 1.1 ± 0.2 µm and 1.3 ± 0.02 µm, respectively. The nucleus was located in the hypotheca. Scanning electron microscope observations revealed that the cells displayed a plate formula of Po, 4′, 6″, 6c, 6s, 5‴ and 2‴, and transmission electron microscope observation demonstrated that the cells contained crystal-like particles. Morphological features indicated that the unspecified Korean isolate belonged to the genus Fukuyoa, and based on the H/W and D/W ratios, the apical pore H/W ratio and thecal pore size, it could be differentiated from other Fukuyoa species. The phylogenetic analyses based on the SSU and LSU rRNA sequences revealed that the

Korean isolate was nested within the genus Fukuyoa with high support, and it grouped with F. cf. yasumotoi isolated from Japan. Based on the morpho-molecular data, a new species, Fukuyoa koreansis sp. nov. is proposed. The maximum growth rate (0.254 d−1) of F. koreansis was observed at 25°C and a salinity of 25. The required levels of temperature and salinity for growth distinguished Fukuyoa koreansis from Gambierdiscus species. Previous article

HIGHLIGHTS

► A new toxic dinoflagellate *Fukuyoa koreansis* was described from Korean coastal waters. ► Based on the height-to-width (H/W) and depth-to- width ratios in cell size, the apical pore H/W ratio and thecal pore size, *Fukuyoa koreansis* could be distinguished from other *Fukuoya* species. ► The phylogenetic position of *Fukuyoa koreansis* was grouped with *F*. cf. *yasumotoi* isolated from Japan and clearly divergent from other *Fukuyoa* species. ► The required temperatures and salinities for growth distinguished *Fukuyoa koreansis* from *Gambierdiscus* species.

Keywords : Gambierdiscus, Growth rate, rRNA, SEM, Toxic dinoflagellate

1. Introduction

The marine epiphytic dinoflagellate genus *Gambierdiscus sensu lato* (*s.l.*), widely distributed in tropical or subtropical coastal waters, is the primary source of ciguatoxin and maitotoxin responsible for ciguatera fish poisoning (CFP; Chinain et al., 2020). CFP is one of the most commonly reported non-bacterial illnesses associated with seafood consumption (Ansdell, 2011; Chinain et al., 2020).

Illness caused by CFP occurs after consumption of fish that have bioaccumulated ciguatoxins through the food web (Bagnis et al., 1980; Laza-Martínez et al., 2016; Rhodes et al., 2014a), which is a concern for local populations dependent on fish consumption in the tropical and subtropical areas (Dickey and Plakas, 2010). Because of the negative impacts on human health, the taxonomy, distribution and ecology of *Gambierdiscus s.l.* are increasingly being studied.

Based on the morphological features and phylogenetic positions, *Gambierdiscus s.l.* encompasses two genera, *Fukuyoa* F.Gómez, D.J.Qiu, R.M.Lopes & Senjie Lin (globular form) and *Gambierdiscus* R.Adachi & Y.Fukuyo (lenticular form) (Gómez et al., 2015; Kuno et al., 2010; Litaker et al., 2009). For *Gambierdiscus,* besides the type species *Gambierdiscus toxicus* R.Adachi & Y.Fukuyo*,* eighteen species have been described (Guiry and Guiry, 2021). The genus *Fukuyoa* was separated from the genus *Gambierdiscus* based on molecular data and lateral compression of cells by Gómez et al. (2015), and it currently comprises three species, namely the type species *Fukuyoa paulensis* F.Gómez, D.J.Qiu, R.M.Lopes & Senjie Lin (Gómez et al., 2015), *F. yasumotoi* (M.J.Holmes) F.Gómez, D.J.Qiu, R.M.Lopes & Senjie Lin and *F. ruetzleri* (M.A.Faust, Litaker, Vandersea, Kibler, W.C.Holland & P.A.Tester) F.Gómez, D.J.Qiu, R.M.Lopes & Senjie Lin (Litaker et al., 2009). The morphological identification of *Fukuyoa* species is extremely difficult, as inter-specific morphological differences among *Fukuyoa* species are very small (Leung et al., 2018). Therefore, molecular techniques play an essential role in further examination of the taxonomic relationships (Gómez et al., 2015; Litaker et al., 2009). In particular, highly conserved molecular markers such as ribosomal RNA (rRNA), including small subunit (SSU) and D1–D3 and D8–D10 regions of large subunit (LSU) rRNA, are most informative for the resolution of relationships between terminal nodes in phylogenetic trees in the taxonomy of *Fukuyoa* and *Gambierdiscus* species (Gómez et al., 2015; Leung et al., 2018; Litaker et al., 2009; Murray et al., 2014).

According to Nishimura et al. (2013), the distribution of *Gambierdiscus s.l.* in Japanese coastal waters displayed clear geographical patterns in subtropical and temperate regions. In coastal waters of Jeju Island, Korea, unidentified *Gambierdiscus* species have been reported (Kim et al., 2011; Baek, 2012), and two other species were identified: *G. caribaeus* Vandersea, Litaker, M.A.Faust, Kibler,

W.C.Holland & P.A.Tester was first reported by Jeong et al. (2012), and a new *Gambierdiscus* species, *G. jejuensis* S.H.Jang & H.J.Jeong was described by Jang et al. (2018). In addition, the effects of temperatures on the growth of these *Gambierdiscus* species were examined to compare with other related species with a global distribution (Jeong et al., 2012; Jang et al., 2018). The taxonomy and toxicity of Korean *Fukuyoa* species, however, have not been investigated, and the distribution of *F. yasumotoi* was reported but lacked detailed information (Shah et al., 2013, 2014).

In a previous publication, an unspecified *Gambierdiscus*-like species, collected off Jeju Island (Korea), was examined to test its toxicity towards the marine copepod *Tigriopus japonicus* Mori (Lee et al., 2014). This species increased the mortality of nauplii and adult females of the marine copepod *T. japonicus*, suggesting that the species may be a ciguatoxin-producing species. However, morpho-molecular data of this *Gambierdiscus*-like species were insufficient for unambiguous identification. For that reason, this unidentified strain reported by Lee et al. (2014) was obtained for this study, and its morphology was examined and molecular phylogeny was constructed based on the nucleotide sequences of almost complete SSU and D1–D3 and D8–D10 regions of LSU rRNA gene. The results showed that this strain clusters within the *Fukuyoa* clade and that it is closely related to a sequence ascribed to *Fukuyoa* cf. *yasumotoi*. Consequently, these findings have led us to propose a new species, *Fukuyoa koreansis* sp. nov.. In addition, we report the growth response of *F. koreansis* to a gradient of temperature and salinity.

2. Materials and methods

2.1. Source of specimens and cultivation

An unspecified *Gambierdiscus*-like species was isolated from seawaters off Jeju Island, Korea (33°13′43″N, 126°36′6″E) during June 2012, and a monoclonal culture established by Dr. Lee, has been maintained in 250 mL Erlenmeyer flask filled with f/2 culture medium at 23°C and 54.05 μmol photons m^{-2} s^{-1} cool-white illumination under a 12L/12D photo-cycle (Lee et al., 2014). The monoclonal culture then was deposited as a strain LIMS-PS-2399 (MABIK PD00002007) in the Library of Marine Samples, Korea Institute of Ocean Science and Technology (KIOST) and was used

for this study.

2.2. Light microscopy

Live cells of strain LIMS-PS-2399 were isolated and photographed at 1000× magnification using an ultra-high-resolution digital camera (DS-Ri2, Nikon, Japan) on an upright microscope (ECLIPSE Ni-E, Nikon, Japan). Chlorophyll *a* autofluorescence was measured with an emission at 630–700 nm and photographed at a 400× magnification using a Zeiss LSM-800 laser scanning confocal microscope (Zeiss, Germany).

2.3. Scanning electron microscopy (SEM)

For SEM, 5 mL of mid-exponential batch cultures were fixed with 2% acidic Lugol's solution (Sigma-Aldrich, Korea) for two hours at room temperature, then rinsed with deionized water. After fixation, the samples were dehydrated in a graded ethanol series (10–99.9% in eight steps) for 15 min at each step. The dehydrated samples were critical-point dried using a critical point dryer (SPI-DRY Regular, SPI Supplies, West Chester, PA) with liquid CO_2. Finally, the samples were coated with platinum and examined using a JEOL JSM 7600F field-emission scanning electron microscope (JEOL Ltd., Tokyo, Japan). The modified Kofoid tabulation nomenclature proposed by Besada et al. (1982) was used in the morphological description.

2.4. Transmission electron microscopy (TEM)

For TEM, the exponentially growing cells were transferred to a 1.5-mL tube and fixed in 2.5% (v/v) glutaraldehyde (final concentration) for 1.5 h, after which the contents of the tube were placed in a 1.5-mL centrifuge tube and concentrated at 2,000×g for 10min. Subsequently, the resulting pellet was transferred to a 1.5-mL tube and rinsed in 0.2 M sodium cacodylate buffer (EMS, Hatfield, PA) at pH 7.4. After several rinses, cells were post-fixed for 1.5 h in 1% (w/v) OsO_4 in deionized H_2O and embedded in agar. Dehydration was performed in a graded ethanol series (50–99.9% in seven steps), and the material was embedded in Spurr's resin (EMS, Hatfield, PA). Sections were prepared on an

EM UC7 ultramicrotome (Leica, Wetzlar, Germany) and stained with 3% (w/v) aqueous uranyl acetate (EMS, Hatfield, PA), followed by lead citrate (Electron Microscopy Sciences). The sections were visualized on a JEOL-1010 TEM (JEOL, Tokyo, Japan) at a voltage of 100kV.

2.5. DNA extraction, PCR and sequencing

Genomic DNA was extracted from 2 mL of exponentially growing culture of the strain LIMS-PS-2399 using the DNeasy® Plant Mini Kit (Qiagen, Valencia, CA) following the manufacturer's instructions. The SSU rDNA sequence was amplified using SR1, SR9, SR4, and SR12b primers (Yamaguchi and Horiguchi, 2005). The amplification of LSU rDNA D1–D3 and D8–D10 regions were performed using D1R and R2 primers (Takano and Horiguchi, 2006), and FD8 and RB primers (Chinain et al., 1999), respectively. The PCR was conducted using Qiagen HotStarTaq Plus polymerase (Qiagen) in a thermal cycler (Mastercycler® nexus; Eppendorf, Germany) with the following conditions: 95°C for 4 min; 35 cycles of denaturation at 94°C for 30 s, annealing at 55°C for 30 s, extension at 72°C for 1 min; and a final elongation at 72°C for 5 min. PCR-amplified products were confirmed by 1% agarose gel electrophoresis. The PCR products were purified with a QIAquick PCR purification kit (Qiagen). The cycle sequencing reaction was performed using the ABI PRISM® Big Dye™ Terminator Cycle Sequencing Ready Reaction Kit (Applied Biosystems, Waltham, MA).

2.6. Sequence alignment and phylogenetic analysis

Sequences were viewed and assembled in DNABaser version 4.36 (http://www.dnabaser.com). Contigs were imported into MEGA version 7.0 (Kumar et al., 2016) and aligned using ClustalW with default settings. Sequence alignments were manually edited using BioEdit version 7.2.5, excluding poorly aligned positions (Hall, 1999). The separate alignments were then checked and concatenated using SequenceMatrix version 1.8 (Vaidya et al., 2011). The final alignment of the concatenated dataset consisted of 34 taxa and 3,590 bp for SSU/LSU(D1–D3)/LSU(D8–D10) (including gaps inserted for alignment). *Alexandrium minutum* (GenBank accession number: JF906998) and

Triadinium polyedricum (KM886380) were used as the outgroups to root the phylogenetic tree.

Phylogenetic trees derived from the sequence dataset were constructed using maximum likelihood (ML) analysis and Bayesian inference, respectively. The ML analysis was carried out using the program RaxML Version 8 (Stamatakis, 2014). The general time reversible (GTR) model with parameters accounting for γ-distributed rate variation across sites (G) was used in all analyses. Bootstrap analysis was carried out for ML with 1,000 resamplings to evaluate statistical reliability. For Bayesian inference, the GTR + I + G substitution model was selected using the Akaike information criterion, as implemented in jModelTest v2.1.4 (Darriba et al., 2012). Bayesian inference was conducted using MrBayes 3.2 (Ronquist et al., 2012), accounting for six-class gamma and one invariant site. Four Markov Chain Monte Carlo chains were run for 10 million generations, sampling every 100 generations. The first 10,000 trees were discarded as burn-in. A majority-rule consensus tree was constructed to examine the posterior probabilities of each clade. The final tree was visualized using MEGA7. To infer the interspecific differentiation, the *p*-distance matrix obtained from the SSU–LSU (D1–D3/D8–D10) rRNA gene sequences was analyzed with a Principal coordinate analysis (PCoA) using the PAST software package version 2.17c (Hammer et al., 2001).

2.7. Effects of temperature and salinity on the growth of *Fukuyoa koreansis*

To obtain subcultures of the cells, the culturing was carried out at 25℃, a salinity of 30, and ca. 100 µmol photons m^{-2} s^{-1} cool-white illumination with a 14L:10D photo-cycle, and the subcultures containing 3,483 cells ml^{-1} were successfully established for the growth experiment. 1 ml of the subculture was transferred into the test tube filled with f/2 medium (G0154; Sigma-Aldrich, St. Louis, MO). Thus, the initial cell density for the growth experiments was 60 cells ml^{-1} (*in-vivo* fluorescence value: 0.98). The effects of temperature and salinity on the growth were examined in triplicate samples. Before the experiments, the cultures were acclimated to each temperature condition. The cultures incubated at 25°C were transferred to various temperature conditions (5, 10, 15, 20, 25 and 30°C), and incubated for five days to acclimate to each temperature condition. After five days of

acclimation, these cultures were used to determine the growth rate at each temperature condition for 30 days. The growth was monitored at two day intervals using an *in-vivo* fluorometer (10-AU; TurnerDesigns, San Jose, CA). The growth rates were examined using a crossed factorial design with 30 combinations of five temperatures (5, 10, 15, 20, 25 and 30℃) and five salinities (15, 20, 25, 30 and 35) levels under ca 100 μmol photons m^{-2} s^{-1} cool-white illumination with a 14L:10D photo-cycle. Salinity levels below 30 were obtained by diluting seawater with deionized water, and salinity of 35 was made by evaporating seawater at 70℃. The regression equation for *in-vivo* fluorescence (FSU) provided a good fit to the observed cell densities; the adjusted r^2 value for *Fukuyoa koreansis* was >0.99 (Appendix S1). Growth rates during the exponential growth phase were calculated using the method of Guillard (1973).

3. Results

3.1. Description of *Fukuyoa koreansis* sp. nov. Zhun Li, J.S.Park, N.S.Kang, K.-W.Lee & H.H.Shin (Figs 1-4)

DIAGNOSIS: Cells are globular in shape, narrow in ventral view and broad in lateral view with a smooth surface, average depth 51.7 ± 4.5 μm (43.1–60.5 μm), width 43.0 ± 4.2 μm (34.4–54.1 μm), and height 55.0 ± 4.7 μm (42.6–64.8 μm), average depth-to-width (D/W) ratio of 1.1 ± 0.2 (0.8–1.2) and height-to-width (H/W) ratio of 1.3 ± 0.02 (1.2–1.4). Epitheca and hypotheca are dome-shaped with the hypotheca slightly longer than the epitheca. Plate formula is Po, 4′, 6″, 6c, 6s, 5‴, 2⁗. Apical pore plate is centrally placed at the apex with a fishhook-shaped apical pore, and is surrounded by a row of marginal pores of nearly equal size. The fishhook-shaped apical pore is horizontally located in apical view. The 4′ and 1′ plates are the largest and smallest apical plates, respectively. Plate 2′ is asymmetrical and more elongated than 3′. The 5″ plate is the largest precingular plate, and the 2″ plate is broad and is larger than 3″ and 4″ plates. The largest postcingular plate is the 2‴ plate. The 2⁗ plate is large, relatively narrow pentagonal and covers the antapex. Thecal pores are round and numerous. Nucleus is located in the hypotheca. The cells contain numerous chloroplasts and crystal-

like particles.

HOLOTYPE: SEM stub 201802F1; deposited at the Library of Marine Samples, Korea Institute of Ocean Science & Technology, Geoje 53201, Republic of Korea. Holotype consists of critical-point dried material from clonal culture LIMS-PS-2399. This strain was sequenced, and the nuclear-encoded SSU, and LSU (D1–D3 and D8–D10 regions) rRNA gene sequences, were deposited in GenBank, with respective accession numbers MH400065, MH400066 and MH464280.

TYPE LOCALITY: Off Jeju Island, Korea (33°13′43″N, 126°36′06″E).

ETYMOLOGY: '*koreansis*' is derived from Korea and refers to the geographic area where the type material was collected.

DISTRIBUTION: Off Jeju Island, Korea; Okinawa, Japan

FURTHER INFORMATION: The strain LIMS-PS-2399, from which the holotype is derived, has also been deposited in the Korean Collection of Type Cultures (KCTC) under strain designation AG60760.

Living cells were globular in shape with an average depth (ventral to dorsal distance) 51.7 ± 4.5 µm (43.1–60.5 µm; n=100), width 43.0 ± 4.2 µm (34.4–54.1 µm; n=100), and height 55.0 ± 4.7 µm (42.6–64.8 µm; n=100), and an average depth-to-width (D/W) ratio of 1.1 ± 0.2 (0.8–1.2; n=55) and height-to-width (H/W) ratio of 1.3 ± 0.02 (1.2–1.4; n=55). Cells were compressed laterally, narrow in the ventral view, broad in lateral view and oval in the apical or antapical view (Fig. 1A-J). Epitheca and hypotheca were dome-shaped, with hypotheca longer than the epitheca (Fig. 1C, D, F). The cingulum was descending and displaced about 2–3 its width (Fig. 1A and C). Apical pore was large and visible using a light microscope (Fig 1G). Cells contained numerous chloroplasts radiating from the interior to the cell periphery (Fig. 1K–M). The nucleus was located in the hypotheca (Fig. 1F).

The thecal surface was smooth (Fig. 4H). Thecal pores were evenly distributed, and round with an average diameter of 0.41 μm (n = 50) (Fig. 4H), and were observed throughout theca plates (Figs 1–2). The cells displayed a plate formula of Po, 4′, 6″, 6c, 6s, 5‴ and 2⁗ (Figs 2–5). The epitheca consisted of 11 plates: apical pore plate (Po), four apical plates, and six precingular plates (Figs. 2A–H, 3A, B). The Po plate was centrally located at the apex, 10–12 μm long and 6–7 μm wide (Figs. 3A, B, 4A–C). Po plate was surrounded by a row of marginal pores of nearly equal size (33–37 pores; n=5) and contained a fishhook-shaped apical pore (8 μm long; n=5) (Figs. 3A, B, 4A–C). The fishhook-shaped apical pore was horizontally placed in the apical view (Fig. 3A, B). The apical pore plate contacted three apical plates: 2′, 3′ and 4′ (Fig. 3A, B). The first apical plate (1′) was quadrangular and contacted three epithecal plates: 4′, 1″ and 6″ plate (Fig. 2A, C). The 4′ plate was the largest plate of the apical series, 20–28 μm long and 17–18 μm wide, with a heptagonal shape, and contacting plates 6″ and 1′ on its posterior side, with plates 2′, 3′ and Po on its anterior side and plates 1″ and 5″ laterally (Figs. 2A, B, 3A, B). Plate 2′ was asymmetrical and more elongated than 3′ (Fig. 3A, B). The suture between 2′ and 3′ was straight in dorso-ventral direction, about 10 μm long, while the suture between 3′ and 4′ was short (Figs. 2G, H, 3A, B). Of the six precingular plates, plate 5″ was the largest, and plate 2″ was larger than plate 4″ (Figs. 2A, B, D, E, 3A, B).

The cingulum was deeply excavated, bordered by narrow lists and contained six narrow plates (Fig. 2I). Plate c2 was the largest cingular plate (Fig. 2I). The sulcus had a deep and narrow excavation (Fig. 2A–C) and consisted of six plates (Fig. 4D–G). The anterior sulcal plate (Sa) had a convex posterior margin and connected to the 1′, 1″ and 6″ plates (Fig. 4D). The right anterior sulcal plate (Sda) was smaller than the left anterior sulcal plate (Ssa) and connected to the cingular plate and Sa plate (Fig. 4D–G). The right posterior sulcal plate (Sdp) and left posterior sulcal plate (Ssp) were lying at the base of the sulcal hollow and were larger than Sda and Ssa, respectively (Fig. 4G). The posterior sulcal plate (Sp) was the largest sulcal plate (about 9 μm long, 5 μm wide and 1.8 H/W ration) and invaded the sulcus with a forked anterior side in contact with the right and left posterior sulcal plates (Figs. 2A, 3C, 4F).

In the hypotheca, there were five postcingular plates and two antapical plates (Figs. 2A–H, 3C,

D). Plate 1‴ was trapezoidal and the smallest of the postcingular plates (Figs. 2C, 3C, D). The largest postcingular plate was the 2‴ plate (covering most of the left part of the hypotheca), followed by the plates 1‴, 3‴, 1⁗, and 2⁗ (Figs. 2C–E, 3C, D). The suture between 2‴ and 2⁗ was about 2–3 times longer than the suture between plates 1⁗ and Sp (Fig. 3C, D). The trapezoidal plate 3‴ was smaller than plates 2‴ and 4‴ and occupied the hypotheca's dorsal part (Fig. 3C, D). Plate 4‴ was pentagonal in shape (Fig. 3C, D). The 5‴ plate was larger than plate 1‴ (Fig. 3C). Furthermore, the pentagonal first antapical plate (1⁗) was small, laid immediately posterior to plate 1‴ and adjacent to Sp, 2‴ and 2⁗ (Figs. 2A, C, 3C). The 2⁗ plate was large, relatively narrow and pentagonal and covered the antapex (Fig. 3C, D). The 2⁗ plate was asymmetrical, and the suture between the 2⁗ and 2‴ plates was longer than the suture between the 2⁗ and 4‴ plates (Fig. 3C, D).

The plate overlap pattern is drawn in Figure 5. The plate overlap in epithecal and hypothecal plate series followed two general gradients: from dorsal to ventral and from the cingulum to the poles. The third precingular (3″) and postcingular (3‴) plates were identified as the keystone plates which overlapped all their adjacent plates (Fig. 5A). The Sp plate was overlapped by all hypothecal plates (Fig. 5B).

TEM sections showed the main ultrastructural features of the cell, such as chloroplasts, crystal-like particles, lipids, mitochondria, nucleus, starch, and trichocysts (Figs. 6A–H). Each chloroplast was bounded by three evenly spaced membranes and each lamella comprised two or three thylakoids (Fig. 6C, H). The nucleus (n) contained several chromosomes (Fig. 6D). The cytoplasm of the cell contained many starch granules (s) and a few lipid droplets (lp) (Fig. 6E). In addition, crystal-like particles (cb) were detected in the cells. They were found within cytoplasmic vacuoles, which were peripherally located inside the cell (Fig. 6E). Numerous mitochondria were distributed all over the cytoplasm of the cell. Oval to elongated mitochondria (m) with tubular cristae and trichocysts were also visible (Fig. 6F). No eyespot was observed. The amphiesma was composed of thecal plates (tp), pellicle (p) and cytoplasmic membrane (cm), external to the cytoplasm (Fig. 6G).

3.2 Molecular phylogeny

The phylogenetic position of *Fukuyoa koreansis* was inferred from SSU–LSU (D1–D3/D8–D10) rRNA gene sequences (Fig. 7). The topologies of the Bayesian-inference and ML phylogenies were congruent, and most clades in the phylogenetic tree received high bootstrap and posterior probability support values. The individual gene trees [SSU, LSU (D1–D3) and LSU (D8–D10)] resulted in a similar pattern as observed from the multiple genes tree (Appendix S1). Genetically, the genus *Fukuyoa* was monophyletic and closely related to *Gambierdiscus* species (Fig. 7).

The molecular phylogenetic analyses revealed that *F. koreansis* clustered together with *F. paulensis*, *F. ruetzleri* and *F. yasumotoi* in a strongly supported clade (Fig. 7), and supported the recognition of *F. koreansis* as a distinct species. In the phylogenetic tree, *F. koreansis* was closest to a Japanese isolate of *F.* cf. *yasumotoi*, with only a very small difference (0.4%) in the concatenated gene sequence distinguishing the two entities. Consequently, these two taxa may be conspecific, although the morphological characteristics of the Japanese isolate of *F.* cf. *yasumotoi* were not described.

The PCoA plots of the uncorrected genetic distance (*p*-distance) based on the SSU–LSU (D1-D3/D8–D10) rRNA gene sequences (3,441bp) showed that *F. koreansis*, *F.* cf. *yasumotoi*, *Fukuyoa* sp. HK Type 1, *F. paulensis*, and a complex group consisting of *F. ruetzleri* and *F. yasumotoi* were classified within four distinct clusters (Fig. 8). The group including *F. koreansis* and *F.* cf. *yasumotoi* was close to the group consisting of *F. ruetzleri* and *F. yasumotoi*. In contrast, it is far away from the other two groups (*F. paulensis* and *Fukuyoa* sp.). The genetic difference between *F. koreansis* and *F. paulensis*, *F. ruetzleri* and *F. yasumotoi* was 1.1–3.5% (Table S1). Among these species, the sequence divergence between *F. koreansis* and *F. yasumotoi* was the lowest (1.1–1.3%). In contrast, the sequence divergence between *F. koreansis* and *Fukuyoa* sp. HK Type 1 was the highest (3.5%). Additionally, *F. koreansis* shared 1.2–1.4% sequence divergence with *F. ruetzleri* and 2.3% with the *F. paulensis*.

3.3 Growth rates of *Fukuyoa koreansis*

The growth rates of the *F. koreansis* at various temperature and salinity combinations are shown in Figure 9 and Table S2. The growth rate ranged from 0 to 0.254 d^{-1} (Fig. 9; Table S2). The

maximum growth rate (0.254 d^{-1}) was obtained at 25 °C and a salinity of 25. In addition, at 25 °C, there were only small differences in the growth rate values between a salinity of 20 and 35, in contrast to zero growth at a salinity of 15 (Table S2). The growth rates were positive at temperatures between 15 °C and 25 °C (Fig. 9). However, *F. koreansis* under relatively low salinity condition (< 20) had a low or negative growth rate. At 15 and 20 °C, *F. koreansis* could grow at all salinities. At the temperatures < 15 °C or 30 °C, cells of *F. koreansis* were ruptured at all salinities.

4. Discussion

4.1 Morphological comparisons of *Fukuyoa* species with its related species

According to Gómez et al. (2015), the genera *Gambierdiscus* and *Triadinium* are morphologically closest to the genus *Fukuyoa*. However, the genus *Fukuyoa* can be distinguished from the genus *Gambierdiscus* by its cell shape in ventral view and relative size of apical plates: the genus *Fukuyoa* is characterized by a globular shape, and plate 4′ is the largest apical plate, whereas the genus *Gambierdiscus* is lenticular in shape and plate 2′ is the largest apical plate. In addition, *Triadinium* species (e.g. *T. polyedricum*) are not highly compressed and are characterized by a rotund shape in apical or antapical views that is not shown in *Fukuyoa* species (Gómez et al., 2015; Shin et al., 2016).

Since the shape, size and plate tabulation in *Fukuyoa* species are important morphological features that can be used to distinguish species (Litaker et al. 2009; Gómez et al. 2015), we compared the Po plate height-to-width (H/W) and the depth-to-width (D/W) ratios of *F. koreansis* with other *Fukuyoa* species such as *F. paulensis*, *F. ruetzleri*, *F. yasumotoi* and an unspecified *Fukuyoa* species (HK type 1) in the phylogenetic tree (Fig. 7 and Table 1). Compared to other *Fukuyoa* species, *F. koreansis* is characterized by a relatively high Po plate H/W (average 2.19) ratio; Po plate H/W ratios of *F. reutzleri* and *Fukuyoa* sp. HK Type 1 are less than 2.1. The depth to width (D/W) ratio of *F. koreansis* is distinctly lower than those of *F. ruetzleri* and *Fukuyoa* sp. HK Type 1. This indicates that the lateral view of *F. koreansis* is more globular in shape than *F. ruetzleri* and *Fukuyoa* sp. HK Type 1. In addition, the sizes of the pores on the cell surface of *F. koreansis* (average diameter 0.41 μm) are

similar to *Fukuyoa* sp. HK Type 1 (average diameter 0.42 mm) and larger than *F. paulensis* (average diameter: 0.35 μm), as documented by Gómez et al. (2015) and Leung et al. (2018). The plate 2′′′′ of *F. koreansis* is long and narrow, whereas *F. paulensis* has a long and broad plate 2′′′′ (Gómez et al., 2015). Regarding cell size and shape, *F. koreansis* seems to be closer to *F. yasumotoi*, than *F. paulensis*, *F. rutzleri* and *Fukuyoa* sp. HK Type 1 (Table 1). Although there are morphological similarities between *F. koreansis* and *F. yasumotoi*, *F. koreansis* can be differentiated from *F. yasumotoi* by the shape of plates 1′ and 2′, and the size of plate 2′′: plate 1′ is quadrilateral in *F. koreansis*, while nearly rectangular in *F. yasumotoi*; plate 2′ of *F. koreansis* is more elongated and occupies a proportionately larger area of the epitheca than in *F. yasumotoi*; the 2′′ plate is clearly smaller than plate 5′′ in *F. koreansis*, but the size of plate 2′′ is similar to the 5′′ plate in *F. yasumotoi* (Litaker et al., 2009). In addition, the height-to-width (H/W) ratio of *F. koreansis* (average 1.3) is higher than *F. yasumotoi* (average 1.21).

According to Litaker et al. (2009) and Nascimento et al. (2015), the size and shape of sulcal plates may be a useful character to distinguish species in *Gambierdiscus s.l.* The genus *Fukuyoa* has no pouch-like vertically-oriented sulcal morphology, and is different from *Gambierdiscus sensu stricto* (=*s.s.*). Plate 1′′′′ of *Gambierdiscus s.s.* is connected to the Sdp and Ssp plates, whereas plate 1′′′′ of *Fukuyoa* species is not connected to the Sdp plate (Litaker et al., 2009; Nascimento et al., 2015). The Sp plate of *F. koreansis* is smaller than *Fukuyoa* sp. HK Type 1 (18.1 μm long, 9.9 μm wide and 1.8 H/W ratio), and narrower than *F. ruetzleri* (13.7 μm long, 9.3 μm wide; and 1.48 H/W ratio) and *F. yasumotoi*, which has a Sp plate wider than that of *F. ruetzleri* (Litaker et al., 2009; Leung et al., 2018).

The plate overlap pattern of *F. koreansis* is generally consistent with other dinoflagellates, following a trend from dorsal to ventral and from equatorial to poles (e.g. Netzel & Dürr, 1984). The third precingular plate of *F. koreansis* is identified as the keystone plate, as previously reported for other *Gambierdiscus s.l.* including *F. paulensis* (Laza-Martinez et al., 2016), *Gambierdiscus excentricus* (Fraga et al., 2011), *G. silvae* (Fraga and Rodríguez, 2014) and *G. toxicus* (Loeblich and Indelicato, 1986; Netzel, 1982). The plate overlap pattern seems to be identical between *Fukuyoa* and

Gambierdiscus.

Of the epiphytic dinoflagellates, the ultrastructure of *Ostreopsis* cf. *ovata* was described by Escalera et al. (2014), however the ultrastructure of *Fukuyoa* and *Gambierdiscus* species has not been examined so far, and in this study the ultrastructure of *F. koreansis* is described for the first time. The structure of the nucleus, chloroplasts, trichocysts and mitochondria of *F. koreansis* were identical to those of other thecate dinoflagellates (e.g. Bibby and Dodge, 1974; Hansen and Moestrup, 1998; Lewis and Burton, 1988), and the crystal-like particles found in *F. koreansis* have been previously reported for many dinoflagellates belonging to different orders, for example, Gonyaulacales (Lewis and Burton, 1988), Peridiniales (Bibby and Dodge, 1974; Calado and Moestrup, 2002) and Suessiales (Craveiro et al., 2010). The crystal-like particles were not observed in *Ostreopsis* cf. *ovata* (Escalera et al., 2014). This indicates that the presence of the crystal-like particles may be useful to distinguish *Fukuyoa* species from other epiphytic dinoflagellates. This highlights that the ultrastructural features of many other epiphytic dinoflagellates should be described and compared.

4.2. Phylogenetic relationships between *F. koreansis* and other *Fukuyoa* species

The phylogenetic analyses based on the SSU and LSU rRNA gene sequences revealed a highly supported *F. koreansis* clade nested within the genus *Fukuyoa*. In addition, *F. koreansis* shows a high similarity in pairwise nucleotide comparison of the SSU and LSU rRNA gene sequences to *F.* cf. *yasumotoi* isolated from Japan (Fig. 8). Although morphological features of *F*. cf. *yasumotoi* were not described in Nishimura et al. (2013), phylogenetic and *p*-distance analyses in this study indicate that the Japanese isolate of *F.* cf. *yasumotoi* and *F. koreansis* are conspecific. Interestingly, our multi-gene phylogeneties revealed that *F. koreansis* displayed a closer genetic resemblance to *F*. *yasumotoi* than *F. ruetzleri*, but the position of the Japanese strain of *F.* cf. *yasumotoi* was unstable in the individual gene trees (e.g., Gómez et al. 2015; Leung et al. 2018). Thus, exploration of multi-gene analyses is necessary, and it will improve the exact bootstrap value of the trees. *F. koreansis* exhibited up to >1.0% genetic difference from other *Fukuyoa* species, indicating that *F. koreansis* is well separated from *F. paulensis, F. ruetzleri* and *F. yasumotoi*. In addition, morphological characters support the

separation of *Fukuyoa* species (section 4.1). In this study, the multi-gene phylogenetics revealed that *F. koreansis* displays a closer genetic resemblance to *F. yasumotoi* than *F. ruetzleri*. However, the clade consisting of *F. koreansis* and *F. yasumotoi* shows a very low support in the phylogenetic analyses. In conclusion, besides the morphological distinction, *F. koreansis* has unique SSU and LSU rRNA gene sequences and the genetic distances are large enough to warrant *F. koreansis* as a new species.

4.3. Growth condition of *Fukuyoa koreansis*

Many previous studies indicated that temperature and salinity play crucial roles in the bloom dynamics and distribution of epiphytic and planktonic dinoflagellates (e.g., Accoroni et al., 2018; Xu et al., 2010; Yoshimatsu et al. 2014). However, the optimal temperature and salinity condition for the growth of *Fukuyoa* species has not been clarified. In the present study, the growth responses to various temperature and salinity conditions of *F. koreansis* are recorded for the first time.

High growth rates in several epiphytic species, some *Gambierdiscus* species (Kibler et al., 2012), *Coolia malayensis* (Morton et al., 1992, reported as *C. monotis*) and *Ostreopsis* cf. *ovata* (Granéli et al., 2011), have been associated with relatively high temperatures (>20°C), and the growth of *F. koreansis* was also enhanced by high temperature (25 °C), however, at 30 °C the cells did not grow, whereas they could survive at 15 °C. This indicates that *F. koreansis* can grow under a wide range of temperatures (between 15 °C and 25 °C) and prefers moderate temperatures for growth.

Based on previous studies, *G. caribaeus* and *G. carpenteri* can survive at or above 30 °C (Yoshimatsu et al., 2014; Kibler et al., 2012; Xu et al., 2016; Tawong et al., 2016), and in addition, *G. jejuensis*, which was isolated from seawaters off Jeju Island (Jang et al., 2018), also grew above 30 °C. This may reflect different temperature preferences between *Gambierdiscus* and *Fukuyoa* species, although there are no reports on the response of other *Fukuyoa* species to high temperature. In addition, under the optimal growth temperatures (15°C and 20°C), *F. koreansis* could survive even at a low salinity level (15). This is in sharp contrast to *Gambierdiscus* species that appear to grow poorly in low salinity waters (< 25 psu) at high water temperatures (25–35 °C) (Kibler et al., 2012; Xu

et al., 2016; Tawong et al., 2016). Consequently, the different responses to water temperature and salinity suggest different ecological niches of *Fukuyoa* and *Gambierdiscus* species.

Occurrences of epiphytic species such as *Gambierdiscus* and *Fukuoya* species have been frequently reported in tropic or subtropic waters (Litaker et al., 2010; Chinain et al., 2020). However, Jeong et al. (2012) isolated *G. caribaeus* at relatively low temperature (14.4 °C), and Jang et al. (2018) reported the growth of *G. jejuensis* at 17.5°C, and *F. koreansis* could also grow at 15 °C. This indicates that the epiphytic species may have an adaptability to the local, temperate environment. Nevertheless, in Korean coastal waters the occurrences of the epiphytic species such as *Gambierdiscus* species have been recorded only in seawaters off Jeju Island. In general, *Gambierdiscus* and *Fukuyoa* species are associated with a benthic macroalgal habitat. This does not favor the expansion of epiphytic species in Korean coastal areas, although Korean temperate waters are favorable for their growth. However, as the global expansion of epiphytic species has been reported (Kibler et al., 2015; Berdalet et al., 2017), the monitoring study of epiphytic species in macroalgal habitat of Korean coastal area is wishful.

Acknowledgments

This work was supported by grants from the Korea Research Institute of Bioscience and Biotechnology (KRIBB) Research Initiative Program, the Efficient Securement of Marine Bioresources and Taxonomic Research funded by the National Marine Biodiversity Institute of Korea (2021M01100), MarineBiotics Project (20210469) and "Techniques development for management and evaluation of biofouling on ship hulls (20210651)" funded by the Ministry of Ocean and Fisheries, Korea. KNM and NC were supported by the PhenoMap project, financed by the French National Research Agency (ANR)

References

Accoroni, S., Ceci, M., Tartaglione, L., Romagnoli, T., Campanelli, A., Marini, M., Giulietti, S., Dell'Aversano, C., Totti, C., 2018. Role of temperature and nutrients on the growth and toxin production of *Prorocentrum hoffmannianum* (Dinophyceae) from the Florida Keys. Harmful Algae 80, 140–148.

Bagnis, R., Chanteau, S., Chungue, E., Hurtel, J.M., Yasumoto, T., Inoue, A., 1980. Origins of ciguatera fish poisoning: a new dinoflagellate, *Gambierdiscus toxicus* Adachi and Fukuyo, definitively involved as a causal agent. Toxicon 18(2), 199–208.

Baek, SH. 2012. Occurrence of the toxic benthic dinoflagellate *Gambierdiscus* spp. in the uninhabited Baekdo Islands off southern coast and Seopsom Island in the Vicinity of Seogwipo, Jeju Province, Korea. Ocean Polar Res 34, 65–71.

Berdalet, E., Tester, P. A., Chinain, M., Fraga, S., Lemee, R., Litaker, W., Penna, A., Usup, G., Vila, M., Zingone A. 2017. Harmful Algal Blooms in Benthic Systems. Oceanography 30, 37–45.

Besada, E., Loeblich, L., Loeblich III, A., 1982. Observations on tropical, benthic dinoflagellates from ciguatera-endemic areas: *Coolia*, *Gambierdiscus*, and *Ostreopsis*. Bull Mar Sci 32(3), 723–735.

Bibby, B.T., Dodge, J.D., 1974. The fine structure of the chloroplast nucleoid in *Scrippsiella sweeneyae* (Dinophyceae). J Ultrastruct Res 48(1), 153–161.

Calado, A.J., Moestrup, Ø., 2002. Ultrastructural study of the type species of *Peridiniopsis*, *Peridiniopsis borgei* (Dinophyceae), with special reference to the peduncle and flagellar apparatus. Phycologia 41(6), 567–584.

Chinain, M., Faust, M.A., Pauillac, S., 1999. Morphology and molecular analyses of three toxic species of *Gambierdiscus* (Dinophyceae): *G.pacificus*, sp nov., *G.australes*, sp nov., and *G.polynesiensis*, sp nov. J Phycol 35(6), 1282–1296.

Chinain, M., Gatti, C.M., Roué, M., Darius, H.T., 2020. Ciguatera-causing dinoflagellates in the genera *Gambierdiscus* and *Fukuyoa*: Distribution, ecophysiology and toxicology. In: Subba Rao, DV (Ed.), Dinoflagellates: Morphology, life history and ecological significance. Nova Science Publishers, New York, pp. 405–457.

Craveiro, S.C., Moestrup, Ø., Daugbjerg, N., Calado, A.J., 2010. Ultrastructure and large subunit rDNA-based phylogeny of *Sphaerodinium cracoviense*, an unusual freshwater dinoflagellate with a novel type of eyespot. J Eukaryot Microbiol 57(6), 568–585.

Darriba, D., Taboada, G.L., Doallo, R., Posada, D., 2012. jModelTest 2: more models, new heuristics and parallel computing. Nat Methods 9(8), 772.

Dickey, R.W., Plakas, S.M., 2010. Ciguatera: A public health perspective. Toxicon 56(2), 123–136.

Escalera, L., Benvenuto, G., Scalco, E., Zingone, A., Montresor, M., 2014. Ultrastructural Features of the Benthic Dinoflagellate *Ostreopsis* cf. *ovata* (Dinophyceae). Protist 165(3), 260–274.

Fraga, S., Rodríguez, F., 2014. Genus *Gambierdiscus* in the Canary Islands (NE Atlantic Ocean) with Description of *Gambierdiscus silvae* sp. nov., a New Potentially Toxic Epiphytic Benthic Dinoflagellate. Protist 165(6), 839–853.

Fraga, S., Rodríguez, F., Caillaud, A., Diogène, J., Raho, N., Zapata, M., 2011. *Gambierdiscus excentricus* sp. nov. (Dinophyceae), a benthic toxic dinoflagellate from the Canary Islands (NE

Atlantic Ocean). Harmful Algae 11, 10–22.

Gómez, F., Qiu, D.J., Lopes, R.M., Lin, S.J., 2015. *Fukuyoa paulensis* gen. et sp nov., a new genus for the globular species of the dinoflagellate *Gambierdiscus* (Dinophyceae). Plos One 10(4).

Granéli, E., Vidyarathna, N.K., Funari, E., Cumaranatunga, P.R.T., Scenati, R., 2011. Can increases in temperature stimulate blooms of the toxic benthic dinoflagellate *Ostreopsis ovata*? Harmful Algae 10(2), 165–172.

Guillard, R.R.L., 1973. Division rates, In: Stein, J.R. (Ed.), Handbook of phycological methods: culture methods and growth measurements. Cambridge University Press, Cambridge, pp. 289–311.

Guiry, M.D., Guiry, G.M., 2021. AlgaeBase. World-wide electronic publication, National University of Ireland, Galway. https://www.algaebase.org; searched on 17 February 2021.

Hall, T.A., 1999. BioEdit: a user-friendly biological sequence alignment editor and analysis program for Windows 95/98/NT. Nucleic Acids Symp Ser 41, 95–98

Hammer, Ø., Harper, D.A.T., Ryan, P.D., 2001. Past: Paleontological Statistics Software Package for Education and Data Analysis. Palaeontologia Electronica 4, 1–9.

Hansen, G., Moestrup, Ø., 1998. Fine-structural characterization of *Alexandrium catenella* (Dinophyceae) with special emphasis on the flagellar apparatus. European Journal of Phycology 33(4), 281–291.

Holmes, M.J., 1998. *Gambierdiscus yasumotoi* sp. nov. (Dinophyceae), a toxic benthic dinoflagellate from southeastern Asia. J Phycol 34(4), 661–668.

Jang, S.H., Jeong, H.J., Yoo, Y.D., 2018. *Gambierdiscus jejuensis* sp. nov., an epiphytic dinoflagellate from the waters of Jeju Island, Korea, effect of temperature on the growth, and its global distribution. Harmful Algae 80, 149–157.

Jeong, H.J., Lim, A.S., Jang, S.H., Yih, W.H., Kang, N.S., Lee, S.Y., Yoo, Y.D., Kim, H.S., 2012. First report of the epiphytic dinoflagellate *Gambierdiscus caribaeus* in the temperate waters off Jeju Island, Korea: morphology and molecular characterization. J Eukaryot Microbiol 59, 637–650.

Kibler, S.R., Litaker, R.W., Holland, W.C., Vandersea, M.W., Tester, P.A., 2012. Growth of eight *Gambierdiscus* (Dinophyceae) species: Effects of temperature, salinity and irradiance. Harmful Algae 19, 1–14.

Kibler, S. R., Tester, P. A., Kunkel, K. E., Moore, S. K., Litaker, R. W. 2015. Effects ofocean warming on growth and distribution of dinoflagellates associated with ciguatera fish poisoning in the Caribbean. Ecol Model 316, 194–210.

Kim, H.S., Yih, W., Kim, J.H., Myung, G., Jeong, H.J. 2011. Abundance of epiphytic dinofalgellates from coastal waters off Jeju Island, Korea during Autumn 2009. Ocean Sci J 46, 205–209.

Kumar, S., Stecher, G., Tamura, K., 2016. MEGA7: Molecular Evolutionary Genetics Analysis

Version 7.0 for Bigger Datasets. Mol Biol Evol 33(7), 1870–1874.

Kuno, S., Kamikawa, R., Yoshimatsu, S., Sagara, T., Nishio, S., Sako, Y., 2010. Genetic diversity of *Gambierdiscus* spp. (Gonyaulacales, Dinophyceae) in Japanese coastal areas. Phycol Res 58(1), 44–52.

Laza-Martínez, A., David, H., Riobó, P., Miguel, I., Orive, E., 2016. Characterization of a strain of *Fukuyoa paulensis* (Dinophyceae) from the Western Mediterranean Sea. J Eukaryot Microbiol 63(4), 481–497.

Lee, K.W., Kang, J.H., Baek, S.H., Choi, Y.U., Lee, D.W., Park, H.S., 2014. Toxicity of the dinoflagellate *Gambierdiscus* sp. toward the marine copepod *Tigriopus japonicus*. Harmful Algae 37, 62–67.

Leung, P.T.Y., Yan, M., Lam, V.T.T., Yiu, S.K.F., Chen, C.Y., Murray, J.S., Harwood, D.T., Rhodes, L.L., Lam, P.K.S., Wai, T.C., 2018. Phylogeny, morphology and toxicity of benthic dinoflagellates of the genus *Fukuyoa* (Goniodomataceae, Dinophyceae) from a subtropical reef ecosystem in the South China Sea. Harmful Algae 74, 78–97.

Lewis, J., Burton, P., 1988. A study of newly excysted cells of *Gonyaulax polyedra* (Dinophyceae) by electron microscopy. British Phycological Journal 23(1), 49–60.

Litaker, R.W., Vandersea, M.W., Faust, M.A., Kibler, S.R., Chinain, M., Holmes, M.J., Holland, W.C., Tester, P.A., 2009. Taxonomy of *Gambierdiscus* including four new species, *Gambierdiscus caribaeus*, *Gambierdiscus carolinianus*, *Gambierdiscus carpenteri* and *Gambierdiscus ruetzleri* (Gonyaulacales, Dinophyceae). Phycologia 48(5), 344–390.

Litaker, R.W., Vandersea, M.W., Faust, M.A., Kibler, S.R., Nau, A.W., Chinain, M., Holmes, M. J., Tester, P. A. Global distribution of ciguatera causing dinoflagellates in the genus *Gambierdiscus*. Toxicon 2010(56), 711–730.

Loeblich, A.R. III, Indelicato, S.R., 1986. Thecal analysis of the tropical benthic dinoflagellate *Gambierdiscus toxicus*. Mar Fish Rev 48, 38–43.

Morton, S.L., Norris, D.R., Bomber, J.W., 1992. Effect of temperature, salinity and light intensity on the growth and seasonality of toxic dinoflagellates associated with ciguatera. J Exp Mar Biol Ecol 157(1), 79–90.

Murray, S., Momigliano, P., Heimann, K., Blair, D., 2014. Molecular phylogenetics and morphology of *Gambierdiscus yasumotoi* from tropical eastern Australia. Harmful Algae 39, 242–252.

Nascimento, S.M., Melo, G., Salgueiro, F., Diniz, B.d.S., Fraga, S., 2015. Morphology of *Gambierdiscus excentricus* (Dinophyceae) with emphasis on sulcal plates. Phycologia 54(6), 628–639.

Netzel, H., 1982. Cytological and ecological aspects of morphogenesis and structure of recent and fossil protist-skeletons: dinoflagellates. Neues Jahrb Geol Palaontol Abh 164, 64–74.

Nishimura, T., Sato, S., Tawong, W., Sakanari, H., Uehara, K., Shah, M.M., Suda, S., Yasumoto, T., Taira, Y., Yamaguchi, H., Adachi, M., 2013. Genetic diversity and distribution of the ciguatera-causing dinoflagellate *Gambierdiscus* spp. (Dinophyceae) in coastal areas of Japan. PLoS One 8(4), e60882.

Rhodes, L., Harwood, T., Smith, K., Argyle, P., Munday, R., 2014a. Production of ciguatoxin and maitotoxin by strains of *Gambierdiscus australes*, *G. pacificus* and *G. polynesiensis* (Dinophyceae) isolated from Rarotonga, Cook Islands. Harmful Algae 39, 185–190.

Rhodes, L., Papiol, G.G., Smith, K., Harwood, T., 2014b. *Gambierdiscus* cf. *yasumotoi* (Dinophyceae) isolated from New Zealand's sub-tropical northern coastal waters. New Zeal J Mar Fresh 48(2), 303–310.

Ronquist, F., Teslenko, M., van der Mark, P., Ayres, D.L., Darling, A., Hohna, S., Larget, B., Liu, L., Suchard, M.A., Huelsenbeck, J.P., 2012. MrBayes 3.2: Efficient Bayesian Phylogenetic Inference and Model Choice Across a Large Model Space. Syst Biol 61(3), 539–542.

Shah, M.M.R., An, S-J., Lee, J-B. 2013. Presence of benthic dinoflagellates around coastal waters of Jeju Island including newly recorded species. J Ecol Environ 36, 347–370.

Shah, M.M.R., An, S-J., Lee, J-B. 2014. Occurrence of sand-dwelling and epiphytic dinoflagellates including potentially toxic species along the coast of Jeju Island, Korea. J Fish Aquat Sci 9, 141–156.

Shin, H.H., Li, Z., Kim, E.S., Youn, J.Y., Jeon, S.G., Oh, S.J., Lim, W.-A., 2016. Morphology and phylogeny of *Triadinium polyedricum* (Pouchet) Dodge (Dinophyceae) from Korean coastal waters. Ocean Science Journal 51(4), 647–654.

Stamatakis, A., 2014. RAxML version 8: a tool for phylogenetic analysis and post-analysis of large phylogenies. Bioinformatics 30(9), 1312–1313.

Takano, Y., Horiguchi, T., 2006. Acquiring scanning electron microscopical, light microscopical and multiple gene sequence data from a single dinoflagellate cell. J Phycol 42(1), 251–256.

Tawong, W., Yoshimatsu, T., Yamaguchi, H., Adachi, M., 2016. Temperature and salinity effects and toxicity of *Gambierdiscus caribaeus* (Dinophyceae) from Thailand. Phycologia 55(3), 274–278.

Vaidya, G., Lohman, D.J., Meier R., 2011. SequenceMatrix: concatenation software for the fast assembly of multi-gene datasets with character set and codon information. Cladistics 27, 171–180.

Xu, N., Duan, S., Li, A., Zhang, C., Cai, Z., Hu, Z., 2010. Effects of temperature, salinity and irradiance on the growth of the harmful dinoflagellate *Prorocentrum donghaiense* Lu. Harmful Algae 9(1), 13–17.

Xu, Y., Richlen, M.L., Liefer, J.D., Robertson, A., Kulis, D., Smith, T.B., Parsons, M.L., Anderson, D.M., 2016. Influence of environmental variables on *Gambierdiscus* spp. (dinophyceae) growth

and distribution. Plos One 11(4), e0153197.

Yamaguchi, A., Horiguchi, T., 2005. Molecular phylogenetic study of the heterotrophic dinoflagellate genus *Protoperidinium* (Dinophyceae) inferred from small subunit rRNA gene sequences. Phycol Res 53(1), 30–42.

Yoshimatsu, T., Yamaguchi, H., Iwamoto, H., Nishimura, T., Adachi, M., 2014. Effects of temperature, salinity and their interaction on growth of Japanese *Gambierdiscus* spp. (Dinophyceae). Harmful Algae 35, 29–37.

Figure legends

Fig. 1. Light micrographs of *Fukuyoa koreansis* sp. nov. (Strain LIMS-PS-2399). (A) High focus of ventral view showing the sulcus and cingulum. (B) Mid focus of ventral view showing the outline of the cell. (C) High focus of ventrolateral view. (D) Mid focus of ventrolateral view. (E) High focus of dorsal view showing the cingulum. (F) Mid focus of dorsal view showing the nucleus (n). (G) High focus of apical view showing the apical pore (arrow). (H) Mid focus of apical view. (I) High focus of antapical view showing the antapical view. (J) Mid focus of antapical showing the shape of the nucleus (n). (K) Confocal images of a cell in dorsal view showing the chlorophyll autofluorescence. (L) Confocal image of ventral view. (M) Confocal image of a cell in lateral view. Scale bars: A–M = 10 μm.

Fig. 2. Scanning electron micrographs (SEM) of *Fukuyoa koreansis* sp. nov. (Strain LIMS-PS-2399). (A, B) Ventral view. (C) Ventral-left lateral view. (D, E) Left lateral view. (F, G) Dorsal-right lateral view.
(H) Right lateral view. (I) Detail of the cingular plates. Small arrows indicate the five sutures separating the six cingular plates (c1–c6). Scale bars: A–I = 10 μm.

Fig. 3. Details of the epithecal and hypothecal plates of *Fukuyoa koreansis* sp. nov. (Strain LIMS-PS-2399) visible in scanning electron micrographs. (A, B) Apical view showing the apical and precingular plates. (C, D) Antapical view showing the antapical and postcingular plates. Scale bars: A–F = 10 μm.

Fig. 4. Details of the apical pore plate, sulcal plates and surface morphology of *Fukuyoa koreansis* sp. nov. (Strain LIMS-PS-2399). (A–B) Thecal external view of apical pore plate. (C) Thecal internal view of apical pore plate. (D–G) Details of the sulcal plates. (H) External view of the theca showing the evenly distributed thecal pores. Scale bars: A–F = 1 μm.

Fig. 5. Schematic drawings of thecal plate patterns of *Fukuyoa koreansis* sp. nov. (A) Epitheca. (B) Hypotheca. (C) Sulcal plates. Arrowheads indicate plate overlap pattern. Abbreviations: n′: apical plate. n″: precingular plate. n‴: postcingular plate. n⁗: antapical plate. Po: apical pore plate. Sa: anterior sulcal plate. Sda: right anterior sulcal plate. Ssa: left anterior sulcal plate. Sdp: right posterior sulcal plate. Ssp: left posterior sulcal plate. Sp: posterior sulcal plate.

Fig. 6. Transmission electron micrographs (TEM) of *Fukuyoa koreansis* sp. nov. (A) Longitudinal section showing several organelles inside the protoplasm: chloroplast (ch) and starch (s). (B) Transversely sectioned cell showing chloroplast (ch), lipid droplets (lp), and nucleus (n). (C–F) TEM micrographs showing the ultrastructure of chloroplast (ch), nucleus (n), crystal-like particle (cb), lipid droplets (lp), starch (s), mitochondria (m), and trichocyst (t). (G) Structure of the amphiesma, which consists of thecal plates (tp), pellicle (p), and cytoplasmic membrane (cm). (H) Three thylakoid lamellae (arrows with numbers). Scale bars: A, B = 5 μm; C–G = 1 μm; H = 0.2 μm.

Fig. 7. Maximum likelihood (ML) tree showing the phylogenetic position of *Fukuyoa koreansis* sp. nov. (in bold) based on SSU+LSU (D1-D3/D8-D10) rRNA gene sequences. *Alexandrium minutum* (GenBank accession number JF906998) and *Triadinium polyedricum* (KM886380) were used as outgroups to root the phylogenetic tree. The numbers on each node are the bootstrap values (%) followed by the Bayesian posterior probability (PP). Only bootstrap values above 50% and PP above 0.7 are shown. The GenBank accession number follows taxon name. Scale bar = 0.05 nucleotide substitutions per site.

Fig. 8. Principal coordinate analysis (PCoA) on the p-distance matrices among sequences of the species of *Fukuyoa*. PCoA based on the SSU–LSU (D1–D3/D8–D10) rRNA gene sequences (3,441bp).

Fig. 9. Contour plots of growth rate (divisions/day) of *Fukuyoa koreansis* under different combinations of salinity and temperature.

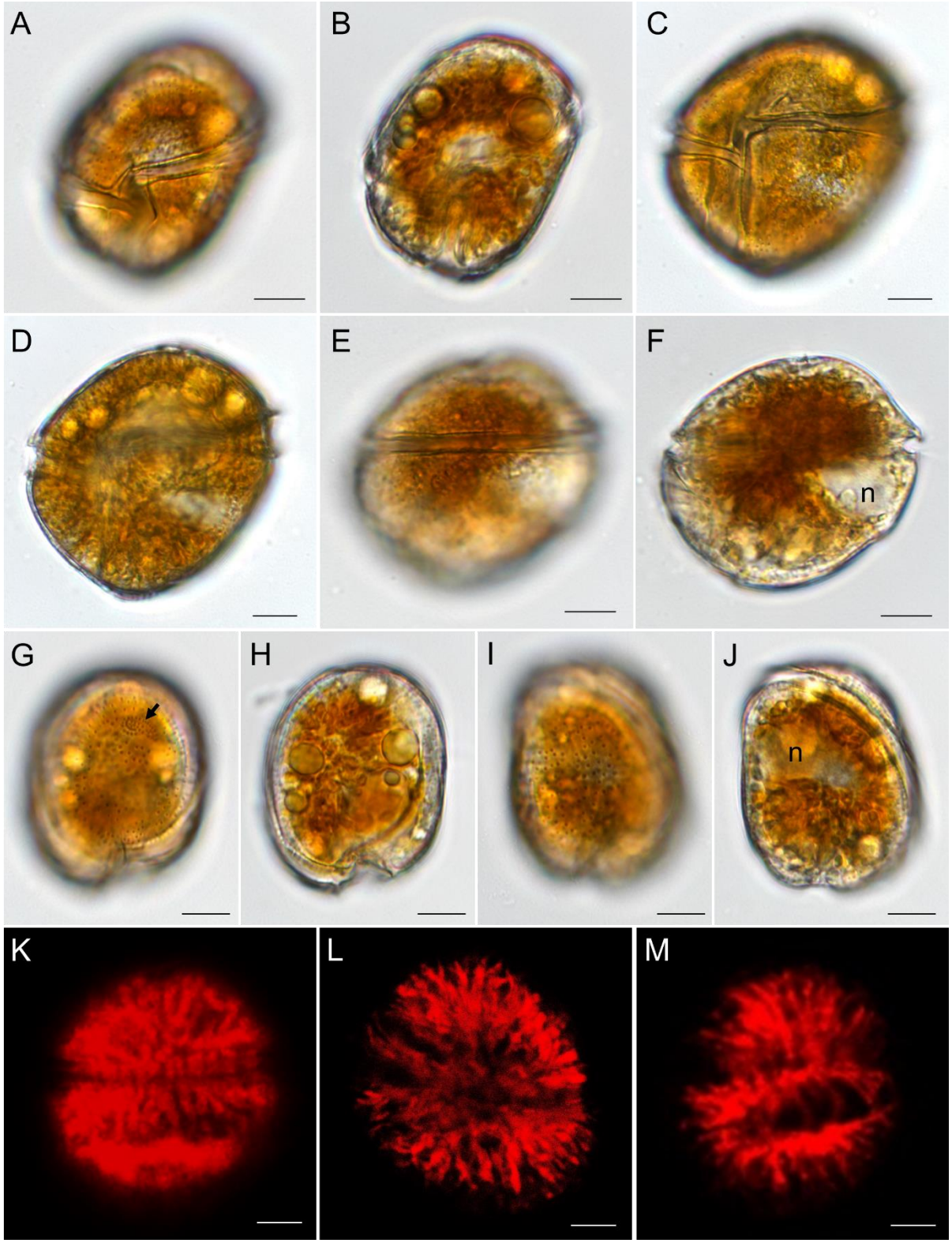

Fig. 1

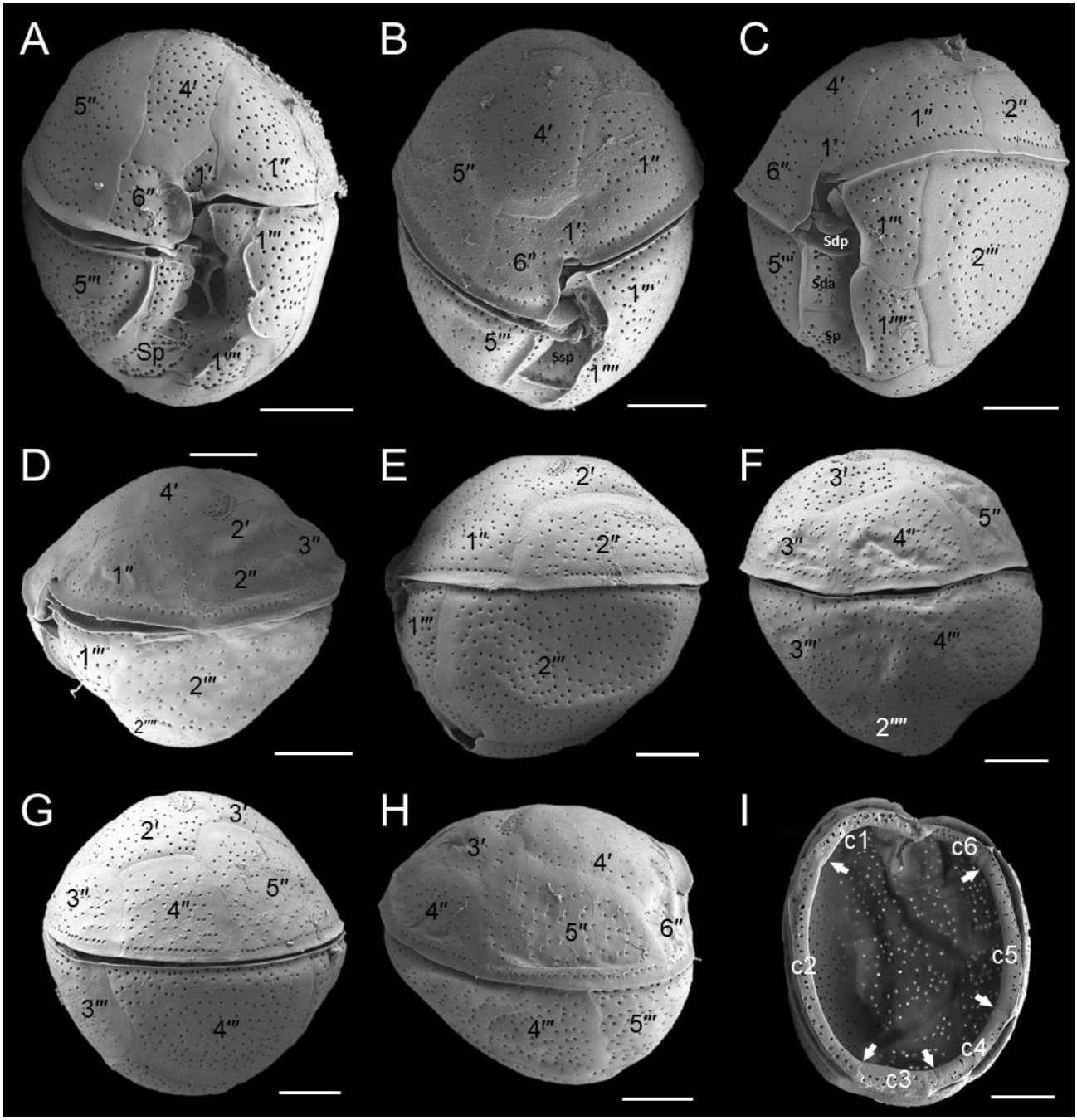
A
5″
4′
1′
1″
6″
1‴
5‴
Sp
1⁗
B
4′
5″
1″
1′
6″
1‴
5‴
Ssp
1⁗
C
4′
1″
2″
1′
6″
Sdp
1‴
5‴
Sda
2‴
Sp
1⁗
D
4′
2′
3″
1″
2″
1‴
2‴
2⁗
E
2′
1″
2″
1‴
2‴
F
3′
5″
3″
4″
3‴
4‴
2⁗
G
2′
3′
3″
4″
5″
3‴
4‴
H
3′
4′
4″
5″
6″
4‴
5‴
I
c1
c6
c2
c5
c4
c3

Fig. 2

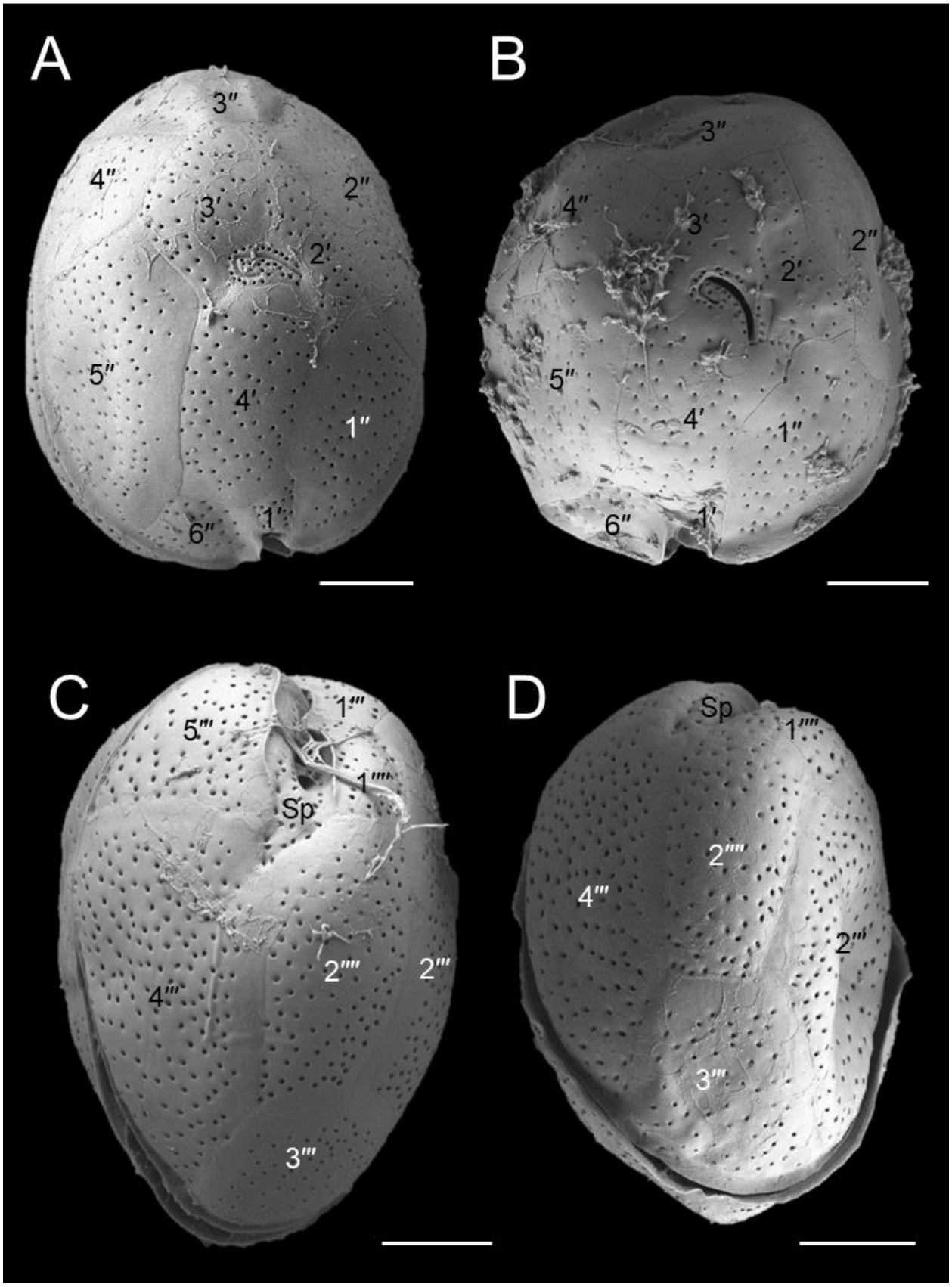

Fig. 3

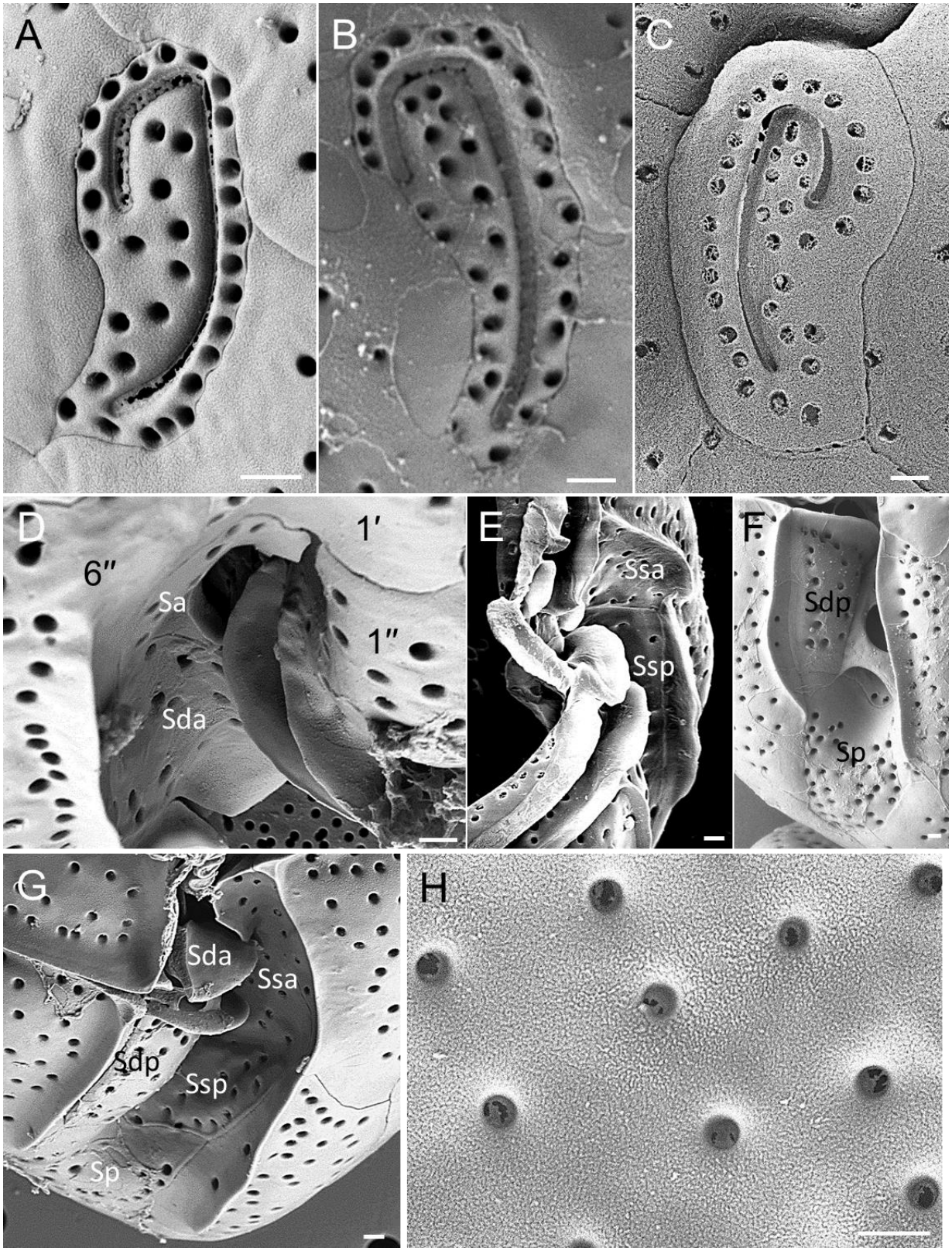

Fig. 4

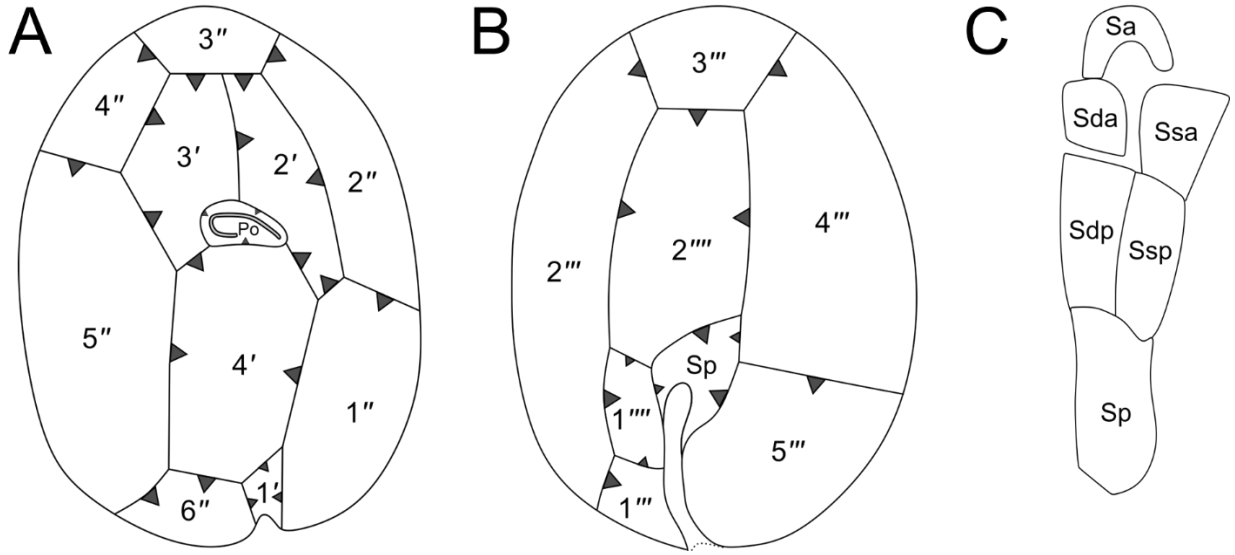

Fig. 5

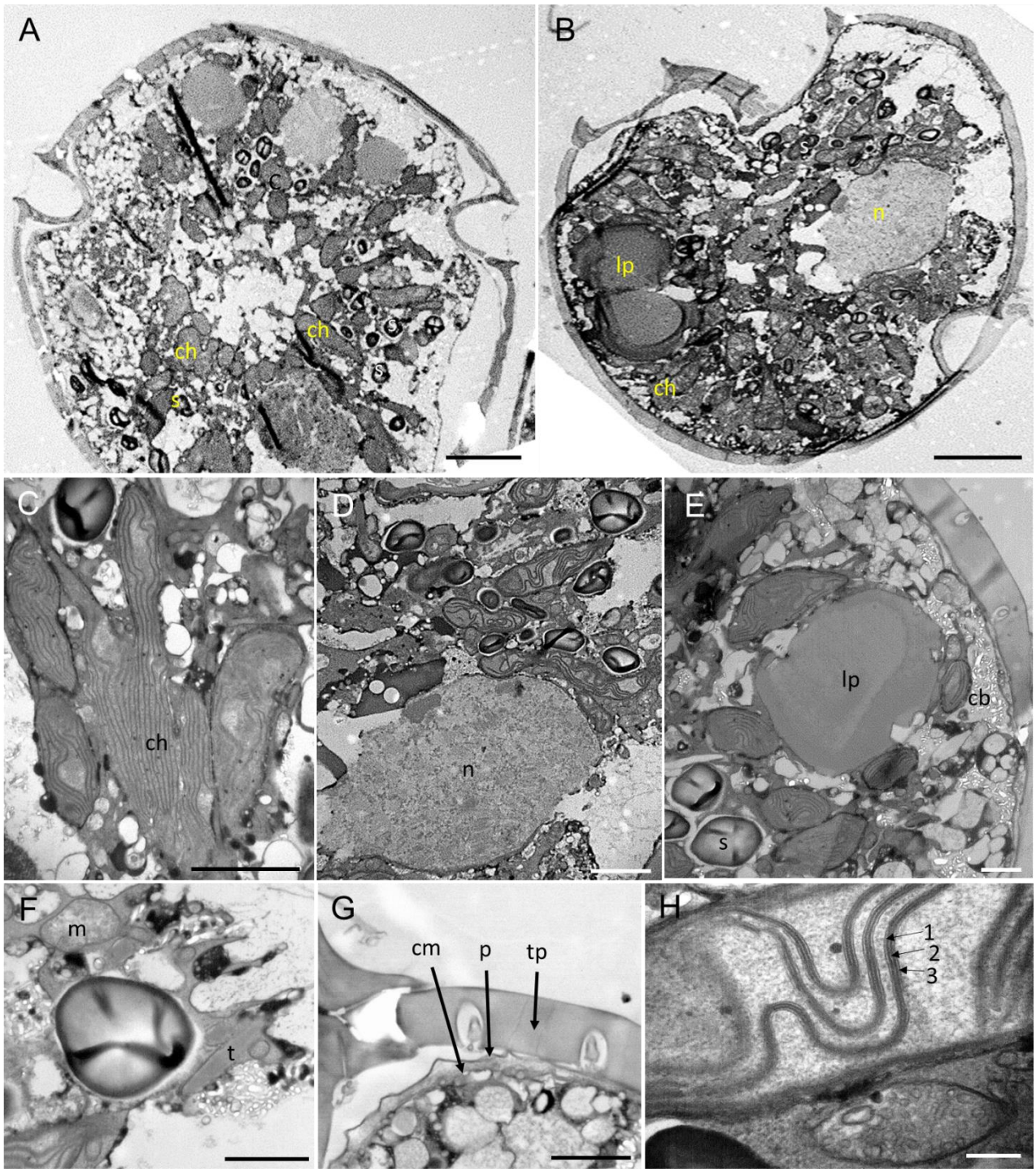

Fig. 6

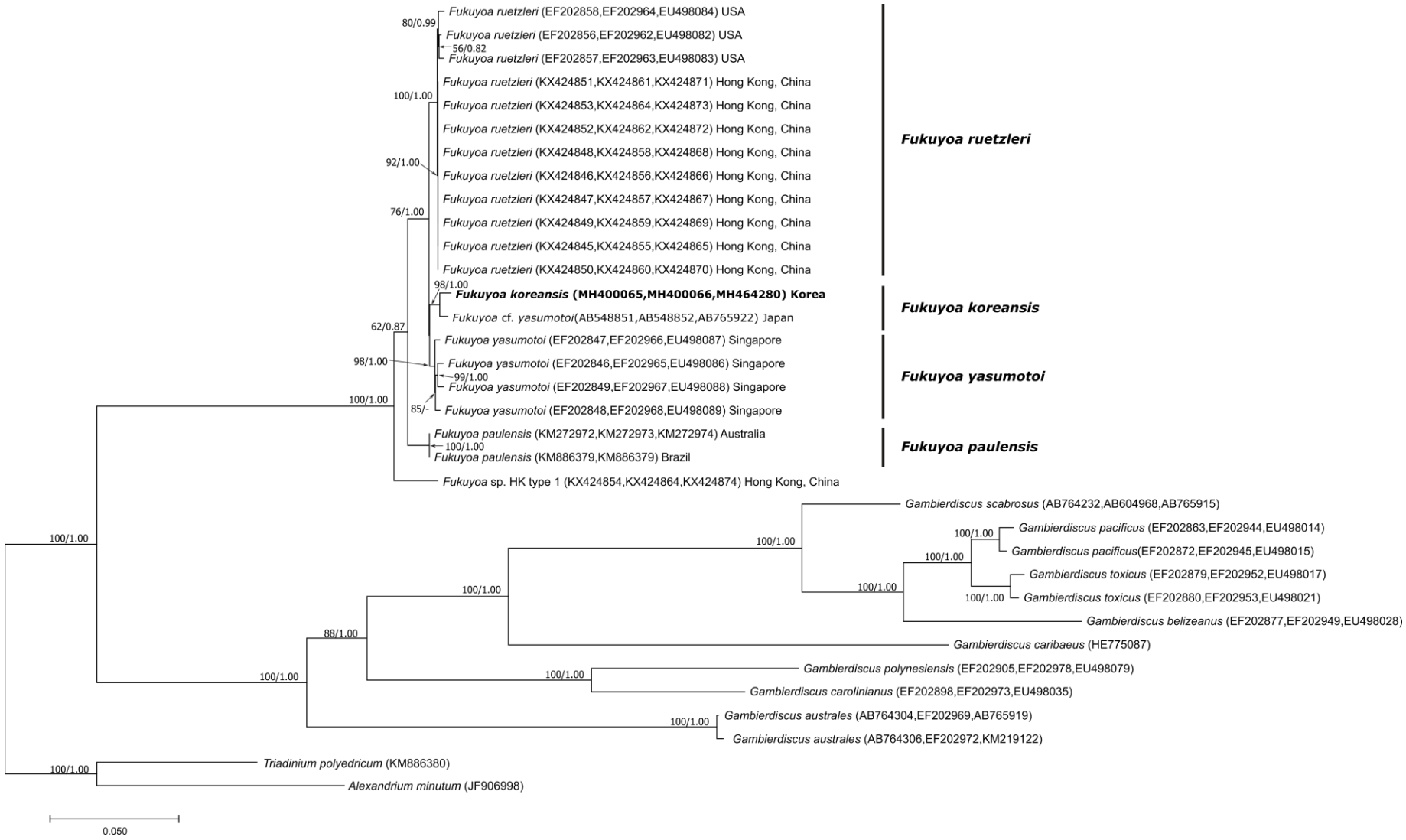
Fukuyoa ruetzleri (EF202858,EF202964,EU498084) USA
Fukuyoa ruetzleri (EF202856,EF202962,EU498082) USA
Fukuyoa ruetzleri (EF202857,EF202963,EU498083) USA
Fukuyoa ruetzleri (KX424851,KX424861,KX424871) Hong Kong, China
Fukuyoa ruetzleri (KX424853,KX424864,KX424873) Hong Kong, China
Fukuyoa ruetzleri (KX424852,KX424862,KX424872) Hong Kong, China
Fukuyoa ruetzleri (KX424848,KX424858,KX424868) Hong Kong, China
Fukuyoa ruetzleri (KX424846,KX424856,KX424866) Hong Kong, China
Fukuyoa ruetzleri (KX424847,KX424857,KX424867) Hong Kong, China
Fukuyoa ruetzleri (KX424849,KX424859,KX424869) Hong Kong, China
Fukuyoa ruetzleri (KX424845,KX424855,KX424865) Hong Kong, China
Fukuyoa ruetzleri (KX424850,KX424860,KX424870) Hong Kong, China
Fukuyoa koreansis (MH400065,MH400066,MH464280) Korea
Fukuyoa cf. yasumotoi(AB548851,AB548852,AB765922) Japan
Fukuyoa yasumotoi (EF202847,EF202966,EU498087) Singapore
Fukuyoa yasumotoi (EF202846,EF202965,EU498086) Singapore
Fukuyoa yasumotoi (EF202849,EF202967,EU498088) Singapore
Fukuyoa yasumotoi (EF202848,EF202968,EU498089) Singapore
Fukuyoa paulensis (KM272972,KM272973,KM272974) Australia
Fukuyoa paulensis (KM886379,KM886379) Brazil
Fukuyoa sp. HK type 1 (KX424854,KX424864,KX424874) Hong Kong, China
Fukuyoa ruetzleri
Fukuyoa koreansis
Fukuyoa yasumotoi
Fukuyoa paulensis
80/0.99
56/0.82
100/1.00
92/1.00
76/1.00
98/1.00
62/0.87
98/1.00
99/1.00
85/-
100/1.00
100/1.00
Gambierdiscus scabrosus (AB764232,AB604968,AB765915)
Gambierdiscus pacificus (EF202863,EF202944,EU498014)
Gambierdiscus pacificus(EF202872,EF202945,EU498015)
Gambierdiscus toxicus (EF202879,EF202952,EU498017)
Gambierdiscus toxicus (EF202880,EF202953,EU498021)
Gambierdiscus belizeanus (EF202877,EF202949,EU498028)
Gambierdiscus caribaeus (HE775087)
Gambierdiscus polynesiensis (EF202905,EF202978,EU498079)
Gambierdiscus carolinianus (EF202898,EF202973,EU498035)
Gambierdiscus australes (AB764304,EF202969,AB765919)
Gambierdiscus australes (AB764306,EF202972,KM219122)
Triadinium polyedricum (KM886380)
Alexandrium minutum (JF906998)
100/1.00
100/1.00
100/1.00
100/1.00
100/1.00
100/1.00
100/1.00
100/1.00
100/1.00
100/1.00
100/1.00
88/1.00
100/1.00
100/1.00
100/1.00
0.050

Fig. 7

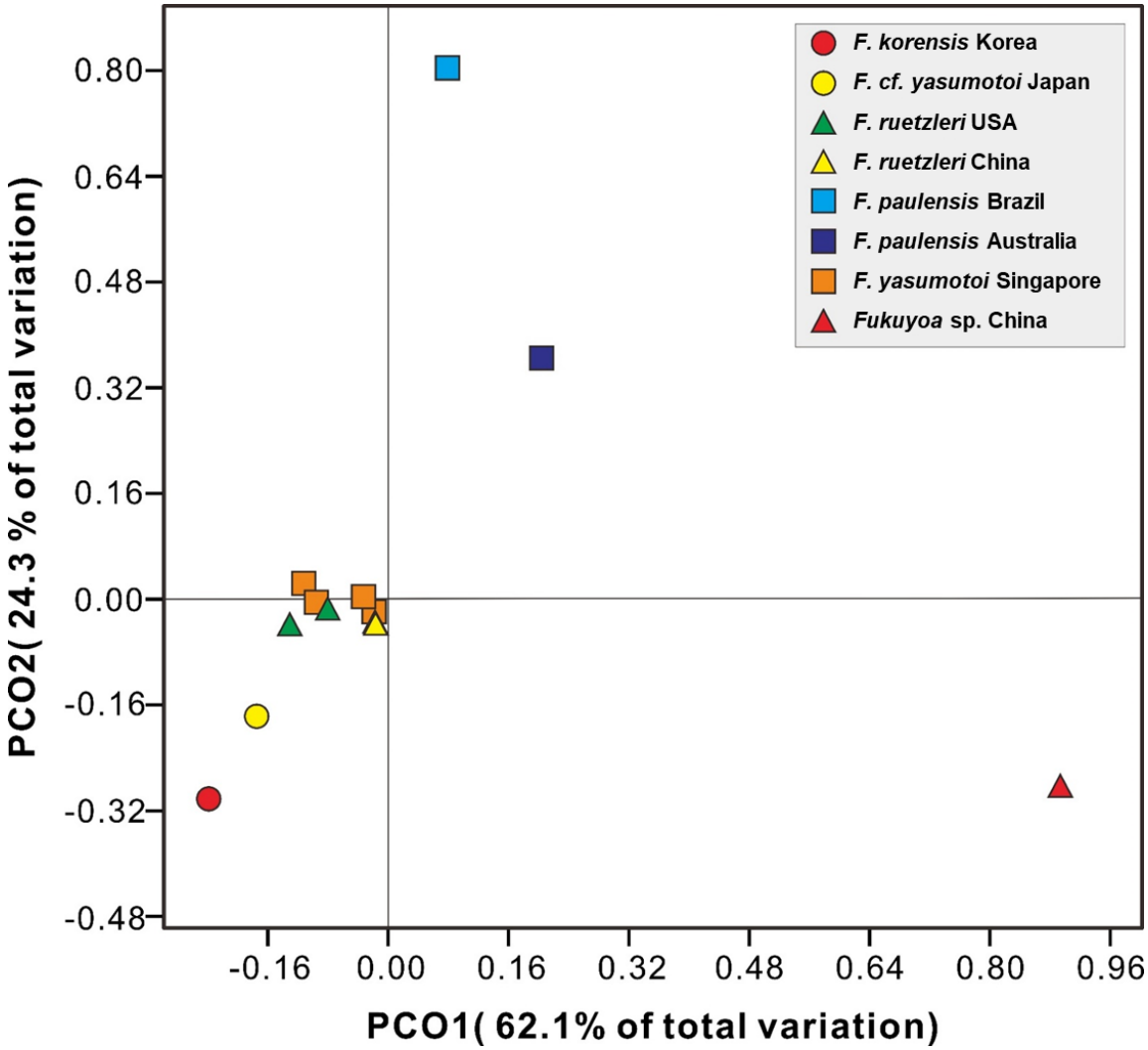
F. korensis Korea
F. cf. yasumotoi Japan
F. ruetzleri USA
F. ruetzleri China
F. paulensis Brazil
F. paulensis Australia
F. yasumotoi Singapore
Fukuyoa sp. China
0.80
0.64
0.48
0.32
0.16
0.00
-0.16
-0.32
-0.48
PCO2(24.3 % of total variation)
-0.16
0.00
0.16
0.32
0.48
0.64
0.80
0.96
PCO1(62.1% of total variation)

Fig. 8

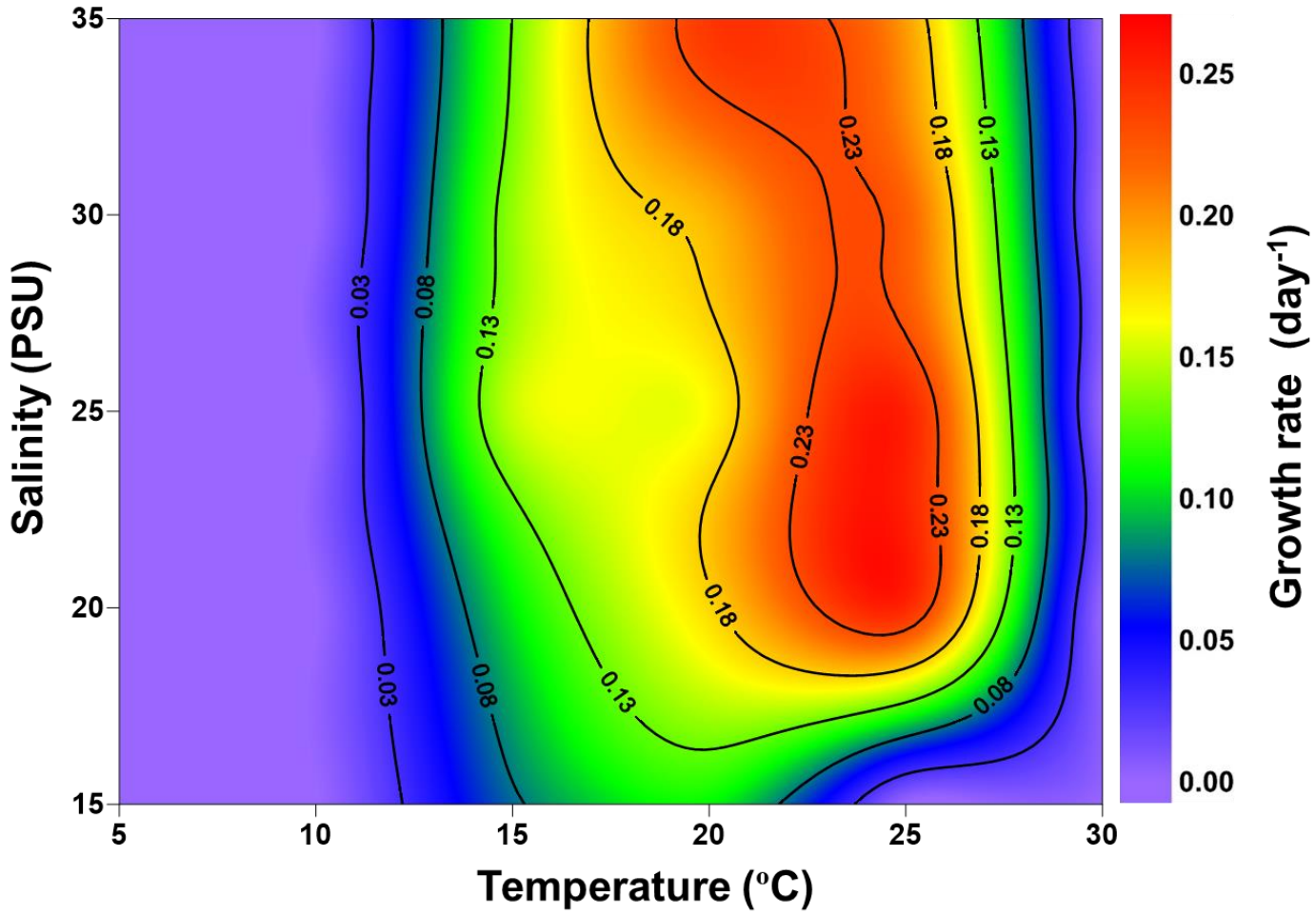
Salinity (PSU)
Temperature (°C)
Growth rate (day-1)
35
30
25
20
15
5
10
15
20
25
30
0.25
0.20
0.15
0.10
0.05
0.00
0.03
0.08
0.13
0.18
0.23

Fig. 9

Table 1. Comparisons of cell morphology and thecal plate dimensions between the species/strains of *Fukuyoa* spp.. “nd”, not determined.

Species	***F. koreansis***	***F. paulensis***				***F. yasumotoi***				***F. reutzleri***		***Fukuyoa sp.* HK Type 1**
Strain	LIMS-PS-2399	Dn135EHU	VGO1185	CAWD210	NQAIF210	nd	Gyasu	nd	nd	SKLMP S044, S051	NOAA8, 22, 25	SKLMP Ve014
Height (H, µm)	55.0 ± 4.7 (42.6–64.8)(n = 79)	48.9 ± 10.9 (35–76) (n = 100)	56.0 ± 3.0 (51–62)	59.8 ± 7.5 (54.3–67.3) (n = 20)	51.0 (49–54)	53.0 ± 0.6 (45–63) (n = 51)	62.4 ± 4.3 (54.4–68.6) (n = 14)	61.7 ± 6.2 (49–70) (n = 20)	62.9 ± 6.8 (55–72) (n = 7)	48.3 ± 4.3 (38.7–60.1) (n = 130)	51.6 ± 4.9 (45.1–59.6) (n = 14)	40.4 ± 4.7 (32.9–53.8) (n = 79)
Depth (D, µm)	51.7 ± 4.5 (43.1–60.5) (n=100)	40.8 ± 8.2 (31–67) (n = 123)	50.0 ± 3.0 (45–56)	54.8 ± 5.7 (49.1–60.5) (n = 20)	49.0 (44–54)	50 ± 1 (43–61) (n = 17)	56.8 ± 5.6 (48.7–66.5) (n = 14)	62.9 ± 4.4 (54–73) (n = 30)	62.6 ± 6.1 (54–71) (n = 7)	48.8 ± 3.5 (40.3–59.3) (n = 155)	45.5 ± 3.3 (41.7–55.0) (n = 12)	40.1 ± 3.1 (33.7–47.7) (n = 85)
Width (W, µm)	43.0 ± 4.2 (34.4–54.1) (n = 79)	30.5 ± 6.6 (24–38) (n = 60)	45.0 ± 2.0 (41–48)	42.5 ± 4.1 (38.4–46.6) (n = 20)	45.0 (40–49)	44 ± 0.8 (38–50) (n = 17)	51.7 ± 5.6 (42.8–60.1) (n = 14)	54.1 ± 5.1 (46–61) (n = 9)	54.7 ± 1.5 (53–56) (n = 3)	38.6 ± 4.0 (28.0–48.5) (n = 176)	35.7 ± 3.0 (30.9–42.2) (n = 12)	32.7 ± 4.6 (23.7–45.2) (n = 79)
D:W ratio	1.1 ± 0.2 (0.8–1.2) (n = 55)	1.29 (n = 48)	~1.2	1.29	1.08	1.14 (n = 17)	1.10	1.28	1.14	1.30 ± 0.08 (1.12–1.63) (n = 105)	1.35	1.36 ± 0.08 (1.19–1.58) (n = 56)
H:W ratio	1.3 ± 0.02 (1.2–1.4) (n = 55)	1.28 (n = 10)	nd	1.41	1.13	nd	1.21	nd	nd	1.27 ± 0.10 (1.03–1.48) (n = 78)	1.45	1.29 ± 0.11 (1.14–1.43) (n = 15)
Apical pore plate (APC)	Central, fishhook-shaped	Curved	Elongated	Elongate ellipsoid	nd	Tear drop shape	Central, long-shark fishhook	Long, curved	Elongated and teardrop shape	Elongated	Elongated	Central, fishhook-shaped
Internal pores of APC	33-37 (n=5)	nd	23–39	nd	nd	33–45	nd	nd	37.1 ± 3.6 (33–42) (n = 8)	29.1 ± 3.2 (22–36) (n = 71)	30 ± 3.7 (22–37) (n = 30)	29.1 ± 3.2 (22–36) (n = 71)
Length of APC (L, µm)	8.9 ± 2.0 (6.7–10.7) (n = 10)	nd	7.63	10–12	nd	8–9	7.6 ± 0.2 (7.0–8.6) (n = 13)	nd	9.2–9.5	7.6 ± 0.4 (6.7–8.4) (n = 19)	8.6 ± 0.5 (7.3–9.2) (n = 18)	7.6 ± 0.4 (6.7–8.4) (n = 19)
Width of APC (W, µm)	4.1 ± 1.2 (2.8–5.1) (n = 10)	nd	4.07	6–7	nd	nd	nd	nd	3.8–4.2	3.8 ± 0.3 (3–4.4) (n = 19)	4.2 ± 0.4 (2.9–4.8) (n = 18)	3.8 ± 0.3 (3–4.4) (n = 19)
L:W ratio of APC	2.19 ± 0.17 (2.08–2.39)	nd	nd	nd	nd	nd	nd	nd	nd	2.01 ± 0.17 (1.81–2.47)	2.09 ± 0.2 (1.8–2.8) (n = 18)	2.01 ± 0.17 (1.81–2.47)

	(n = 10)									(n = 19)		(n = 19)
Sp plate	Forked and to the sulcus, larger	Forked and invaded the sulcus	Forked and invaded the sulcus	nd	Forked and invaded the sulcus	nd	Forked and invaded the sulcus, larger	Forked and invaded the sulcus	Large and fork-shaped	Six side, forked, narrow, invades sulcus	Six side, forked, narrow, invades sulcus	Six side, forked, narrow, invades sulcus
Reference	This study	Laza-Martínez et al. (2016)	Gómez et al. (2015)	Rhodes et al. (2014a,b)	Murray et al. (2014)	Holmes (1998)	Litaker et al. (2009)	Saburova et al. (2013)	Saburova et al. (2013)	Leung et al. (2018)	Litaker et al. (2009)	Leung et al. (2018)